# Perfect Static Balance of Linkages by Addition of Springs But Not Auxiliary Bodies

**Sangamesh R. Deepak**
e-mail: sangu@mecheng.iisc.ernet.in

**G. K. Ananthasuresh**
e-mail: suresh@mecheng.iisc.ernet.in

Department of Mechanical Engineering,
Indian Institute of Science,
Bangalore 560012, India

*A linkage of rigid bodies under gravity loads can be statically counter-balanced by adding compensating gravity loads. Similarly, gravity loads or spring loads can be counter-balanced by adding springs. In the current literature, among the techniques that add springs, some achieve perfect static balance while others achieve only approximate balance. Further, all of them add auxiliary bodies to the linkage in addition to springs. We present a perfect static balancing technique that adds only springs but not auxiliary bodies, in contrast to the existing techniques. This technique can counter-balance both gravity loads and spring loads. The technique requires that every joint that connects two bodies in the linkage be either a revolute joint or a spherical joint. Apart from this, the linkage can have any number of bodies connected in any manner. In order to achieve perfect balance, this technique requires that all the spring loads have the feature of zero-free-length, as is the case with the existing techniques. This requirement is neither impractical nor restrictive since the feature can be practically incorporated into any normal spring either by modifying the spring or by adding another spring in parallel.*
[DOI: 10.1115/1.4006521]

## 1 Introduction

A linkage is said to be statically balanced if it is in static equilibrium in *all its* configurations. In this paper, all the loads on a linkage are assumed to be conservative. Hence, static balance is equivalent to invariance of the net potential energy of all the loads with respect to all configurations of the linkage. This paper gives a new technique to statically balance a revolute-jointed linkage loaded by constant forces (e.g., gravity) and/or zero-free-length springs. Although the technique is detailed in this paper for planar linkages, it extends to *spatial* spherical and/or revolute-jointed linkages.

The need for static balance of gravity loads in structures and machines is well known. Hence, a number of techniques are developed for static balance of gravity loads [1–4]. The need for static balance of inherent spring loads is not as common. This need is particularly felt in compliant mechanisms where an elastically deformable structure is used but its stiffness is not always desired. This work is motivated by such practical applications.

Techniques in the literature for static balancing a loaded linkage may be classified into approximate balancing techniques and perfect balancing techniques. The perfect balancing techniques can be further subdivided into

Category 1: Both original loads and balancing loads are constant weights.
Category 2: Original loads are constant weights and balancing loads are *zero-free-length* spring loads.
Category 3: Both original and balancing loads are *zero-free-length* spring loads.

These categories are illustrated in Fig. 1. The top row of Fig. 1 shows these categories for a lever. While the static balance of a lever in category 1 is known for a long time, the balancing of a lever under categories 2 and 3 was discovered relatively recently, as would be evident from the literature survey given later. The bottom row of Fig. 1 shows these categories for a multibody linkage. For multibody revolute-jointed linkages, static balancing techniques are known only for categories 1 and 2. Furthermore, for multibody linkages under category 2, beyond 3R serial linkage, all the methods reported so far in the literature use auxiliary bodies. The bottom row of Fig. 1 under category 2 illustrates one such reported method [2] where auxiliary bodies are highlighted in gray color.

This paper deals with perfect static balancing of multibody revolute-jointed linkages. It shows that just as balancing under category 1 can be done without auxiliary bodies, balancing under categories 2 and 3 can also be done without using auxiliary bodies. The background for this work is presented next.

**1.1 Zero-Free-Length Springs and Perfect Static Balancing.** Zero-free-length springs, in contrast to normal springs, have zero-length between its endpoints when the spring force is zero. When a spring is anchored to two bodies having relative motion, the spring force as a function of its two anchor points is of interest. As illustrated in Fig. 2, this function happens to be linear in a zero-free-length spring but nonlinear in a positive-free-length spring inspite of both springs having a linear force-deflection relationship. Appendix A shows that the nonlinearity associated with nonzero-free-length springs prevents

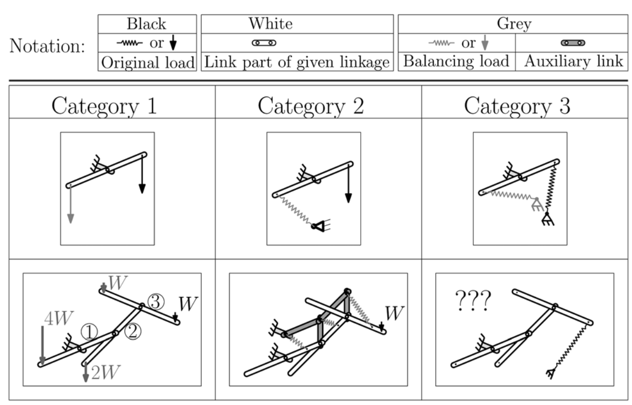


**Fig. 1 Three categories of perfect static balancing techniques shown on a lever and a multibody linkage**

Contributed by the Mechanisms and Robotics Committee of ASME for publication in the Journal of Mechanisms and Robotics. Manuscript received February 26, 2011; final manuscript received February 22, 2012; published online April 25, 2012. Assoc. Editor: Frank C. Park.

  

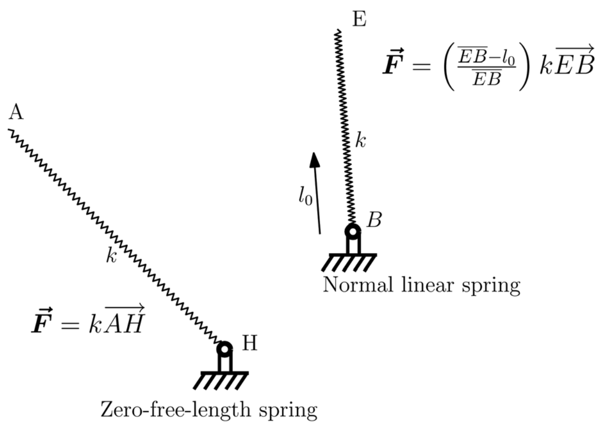


**Fig. 2 Difference between zero-free-length spring and normal spring**

perfect static-balance when only normally available positive-free-length springs are present. Herder [5] has documented a few practical arrangements to decrease the free-length of a normal spring all the way to zero and even to a negative value.

If a normal positive-free-length spring cannot be incorporated into any of the arrangements of Herder [5], as is the case with loading springs, then by adding an appropriate negative-free-length spring in parallel to it, a zero-free-length spring can be realized out of both of them. In this way, even normal spring loads can be brought under the ambit of techniques under category 3. Thus, the technique presented in this paper is practical and general enough to handle normal spring loads in addition to weights and zero-free-length spring loads.

### 1.2 Literature Survey

*1.2.1 Perfect Static Balancing of a Lever.* The three categories of perfect static balancing of a lever can be seen in Fig. 1. The technique under category 1 is known from historic times and is popularly known as the lever principle of Archimedes. The discovery of zero-free-length springs and the technique under category 2 are credited to Lucien LaCoste (see Ref. [1]). We consider this discovery to be ground-breaking since it showed for the first time that a weight can be statically balanced by a spring. Recently, using a differential bevel gear, this technique is adapted for static balancing a body having the spatial roll and pitch motion about a point [6]. The techniques under category 3 for a lever are discussed in detail by Herder [5].

*1.2.2 Perfect Static Balancing of a Multibody Linkage.* Most of the static balancing techniques for multibody linkages under category 1 have been known for a long time. The technique shown in Fig. 1 under category 1 is one such. Another example of the techniques under this category is in Ref. [7].

Under category 2, Streit and Shin [2] showed that in principle any planar linkage loaded by gravity loads can be balanced using zero-free-length springs. They also provided a different technique to statically balance serial revolute-jointed planar linkages. It is this technique that is illustrated using three-revolute-jointed linkage in Fig. 1 under category 2. The same work also provides another technique for a linkage with revolute-slider joint pairs. Although Streit and Shin [2] provide techniques for planar linkages, the techniques can be extended to spatial linkages. Rahman et al. [8] provide one such extension to anthropomorphic robots. Recent work on static balancing of spatial linkages includes that of Lin et al. [9]. References [3] and [4] provide a different class of techniques under category 2 for revolute-jointed linkages. All these techniques use auxiliary bodies in addition to extra zero-free-length springs.

Under category 3, for a multibody linkage, there is a technique which is applicable only for a four-bar linkage and a two-revolute-jointed linkage [10]. Later, we recognized two more methods for the same linkages in Ref. [11].

Under categories 2 and/or 3, Refs. [12] and [13] as well as a method in Ref. [11] do not use auxiliary links. The current paper has evolved out of Ref. [12] and allows a more general class of solutions in comparison to Ref. [12]. Reference [13] derives equations governing static balance of gravity loaded 2R and 3R linkages and provides solutions to the equations without using auxiliary links.

*1.2.3 Other Static Balancing Techniques.* Among the balancing techniques outside the ambit of the aforementioned three categories, most are approximate balancing techniques and a few, although perfect balancing techniques using ordinary springs, use cams and pulleys to modulate the behavior of springs. Further, all those techniques balance against gravity loads. Agrawal and Agrawal [14] presented an approximate static balancing method using nonzero-free-length springs. Gopalswamy et al. [15] gave an approximate static balancing technique where torsional springs were used as balancing elements. There is a lot of literature on static balancing of parallel manipulators and one such work is Ref. [16]. The balancing techniques that modulate the behavior of springs include the techniques in Refs. [17] and [18], where a pulley of varying radius was used, and the technique in Ref. [19], where a cam was used.

### 1.3 Practical Relevance.

The utility of techniques under category 2 is well recognized. These techniques are applied in static balancing of robots, anglepoise lamps, and flight simulators. If a robot or a flight simulator is statically balanced, then the actuators do not have to work against the gravity loads acting on the links of the robot or the cockpit of flight simulator. This greatly reduces the force/torque requirement of the actuators and also supposedly makes the actuator control easy. Further, an advantage of balancing techniques in category 2 over category 1 is that the inertia added to the linkage is minimal. The new technique that this paper presents under this category will provide one more option to a designer seeking to statically balance linkages under gravity loads using springs.

The utility of any technique under category 3 is not direct. There are hardly any practical problems where a linkage under zero-free-length springs is required to be statically balanced against it. However, there are situations where a linkage under elastic loads other than the zero-free-length spring loads is required to be balanced. For example, the balancing of the elastic forces of a cosmetic covering in a hand prosthesis (see Refs. [10] and [20]) and the inherent elastic forces in a compliant mechanism (see Ref. [21]) is desired. Unlike in a hand prosthesis, there is no inherent linkage in a compliant mechanism, which is a monolithic elastic piece that transmits force or motion by virtue of elastic deformation. However, it is established that compliant mechanisms with flexural joints and certain kinds of slender segments can be modeled as rigid-linkages with torsional springs and tension springs (see Refs. [22] and [23]). Since the perfect static balance of these types of elastic forces on linkages is not demonstrated, one would look for a good approximate static balance. If such elastic forces are approximately modeled as zero-free-length springs, then the techniques under category 3 would offer insights and also a starting point for optimization techniques to balance such elastic loads.

### 1.4 Organization of the Paper.

In order to show the features of zero-free-length springs and constant loads that make perfect static balance possible with them, perfect static balance of one of the simplest linkages: a rigid body on a fulcrum, i.e. a lever, is discussed in Sec. 2. Section 3 shows that even though the principles of static balance of a lever can be extended to a rigid body freely moving in a plane, static balancing the translation component of the rigid body is not possible in most practical conditions. Based on a result in Sec. 3, it is shown in Sec. 4 that an assemblage of

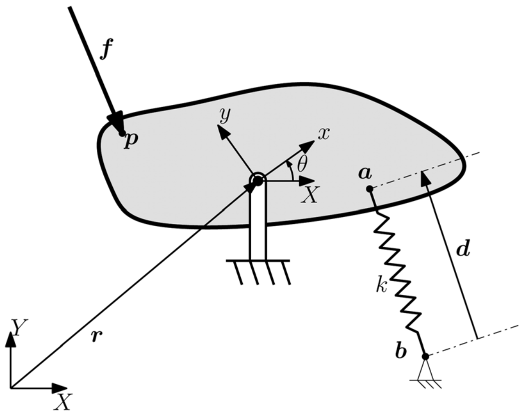


**Fig. 3 A lever under a constant load and a spring load**

rigid bodies in a plane with zero-free-length spring and constant load interactions between the bodies can always be statically balanced if the assemblage forms a revolute-jointed linkage. Section 5 argues that the technique for planar revolute-jointed linkages extends for spatial spherical and/or revolute-jointed linkages. Concluding remarks are in Sec. 6.

## 2 Balancing a Lever

Consider a lever pivoted to the ground, as shown in Fig. 3. The configuration of the lever with respect to the global frame of reference $(X - Y)$ can be described by $\theta$, which is the angle from the global frame to the local frame of reference of the lever.

Figure 3 also shows two kinds of load: (1) a spring attached between a point of the lever and a point of the global frame and (2) a constant force acting at a point on the lever. Here, a constant force means that the force has a constant direction *with respect to the global frame* and a constant magnitude. A complete specification of the spring load would involve (1) the spring constant, denoted by $k$, (2) the local coordinate of the anchor point on the lever, denoted by $\boldsymbol{a} = [a_x\ a_y]^T$, and (3) the global coordinate of the anchor point on the global reference frame, denoted by $\boldsymbol{b} = [b_x\ b_y]^T$. A complete specification of the constant force would involve (1) the force components with respect to the global frame, denoted by $\boldsymbol{f} = [f_x\ f_y]^T$, and (2) the local coordinate of the point of action of the force on the lever, denoted by $\boldsymbol{p} = [p_x \quad p_y]^T$.

**2.1 Potential Energy as a Function of the Configuration Variable.** By referring to Fig. 3, the potential energy of the constant load is

$$PE_c = -\boldsymbol{f}^T(\boldsymbol{r} + \boldsymbol{R}(\theta)\boldsymbol{p}) \tag{1}$$

where $\boldsymbol{r} = [r_x\ r_y]^T$ is the coordinate of the origin of the local frame on the lever with respect to the global frame and $\boldsymbol{R}$ is the rotation matrix function given by

$$\boldsymbol{R}(\psi) = \begin{bmatrix} \cos\psi & -\sin\psi \\ \sin\psi & \cos\psi \end{bmatrix} \quad \text{for any angle } \psi \tag{2}$$

The potential energy of the spring is

$$PE_s = \frac{k}{2}(l - l_0)^2 = \frac{k}{2}l^2 - kl_0 l + \frac{k}{2}l_0^2 \tag{3}$$

where $l_0$ is the free length of the spring and $l$ is the magnitude of $\boldsymbol{d}$, the displacement of one-end point of the spring with respect to the other. This $\boldsymbol{d}$, referring to Fig. 3, is

$$\boldsymbol{d} = (\boldsymbol{r} + \boldsymbol{R}(\theta)\boldsymbol{a}) - \boldsymbol{b} \tag{4}$$

Since $l^2 = \boldsymbol{d}^T\boldsymbol{d}$, the potential energy in expression (3) may be rewritten as

$$PE_s = \frac{k}{2}\boldsymbol{d}^T\boldsymbol{d} - kl_0\sqrt{\boldsymbol{d}^T\boldsymbol{d}} + \frac{k}{2}l_0^2 \tag{5}$$

If the free-length of the spring is zero, then only the first term in Eq. (5) remains and hence, we call it as $PE_{s,\text{zero}}$, i.e.

$$\begin{aligned} PE_{s,\text{zero}} &= \frac{k}{2}\boldsymbol{d}^T\boldsymbol{d} = \frac{k}{2}((\boldsymbol{r} + \boldsymbol{R}(\theta)\boldsymbol{a}) - \boldsymbol{b})^T((\boldsymbol{r} + \boldsymbol{R}(\theta)\boldsymbol{a}) - \boldsymbol{b}) \\ &= \frac{k}{2}(\boldsymbol{r}^T\boldsymbol{r} + \boldsymbol{a}^T\boldsymbol{R}^T(\theta)\boldsymbol{R}(\theta)\boldsymbol{a} + \boldsymbol{b}^T\boldsymbol{b} - 2\boldsymbol{r}^T\boldsymbol{b} + 2\boldsymbol{r}^T\boldsymbol{R}(\theta)\boldsymbol{a} \\ &\quad - 2\boldsymbol{b}^T\boldsymbol{R}(\theta)\boldsymbol{a}) \\ &= \frac{k}{2}\left(\boldsymbol{r}^T\boldsymbol{r} + \boldsymbol{a}^T\boldsymbol{a} + \boldsymbol{b}^T\boldsymbol{b} - 2\boldsymbol{r}^T\boldsymbol{b} + 2\boldsymbol{r}^T\boldsymbol{R}(\theta)\boldsymbol{a} - 2\boldsymbol{b}^T\boldsymbol{R}(\theta)\boldsymbol{a}\right) \\ &\quad \because\ \boldsymbol{R}^T(\theta)\boldsymbol{R}(\theta) = \boldsymbol{I} \end{aligned} \tag{6}$$

Since the remaining last two terms of the potential energy in Eq. (5) are nonzero only if free-length $l_0$ is nonzero, we name these terms as $PE_{s,\text{nonzero}}$, i.e.

$$PE_{s,\text{nonzero}} = -kl_0\sqrt{\boldsymbol{d}^T\boldsymbol{d}} + \frac{k}{2}l_0^2 \tag{7}$$

From Eq. (6), it follows that $\boldsymbol{d}^T\boldsymbol{d} = \frac{2}{k}PE_{s,\text{zero}}$. Substituting this in Eq. (7) leads to the following expression for $PE_{s,\text{nonzero}}$.

$$PE_{s,\text{nonzero}} = -l_0\sqrt{2kPE_{s,\text{zero}}} + \frac{k}{2}l_0^2 \tag{8}$$

In the expressions of the potential energy in Eqs. (1), (6), and (8), as the configuration of the lever varies, $\boldsymbol{f}$, $\boldsymbol{p}$, $\boldsymbol{a}$, $\boldsymbol{b}$, $k$, $l_0$ remain constants and $\boldsymbol{r}$ is made a constant by choosing the origin of the local frame on the lever to coincide with the pivot point. The dependency of the expressions on the configuration is due the matrix $\boldsymbol{R}(\theta)$ which, by examining the definition of $\boldsymbol{R}$ in Eq. (2), can be split as

$$\boldsymbol{R}(\theta) = \begin{bmatrix} 1 & 0 \\ 0 & 1 \end{bmatrix}\cos\theta + \begin{bmatrix} 0 & -1 \\ 1 & 0 \end{bmatrix}\sin\theta = \boldsymbol{I}\cos\theta + \boldsymbol{R}\left(\frac{\pi}{2}\right)\sin\theta \tag{9}$$

This form of $\boldsymbol{R}(\theta)$ indicates that $PE_c$ in Eq. (1) and $PE_{s,\text{zero}}$ in Eq. (6) can be written as a linear combination of $\sin\theta$, $\cos\theta$, and 1 (for constants). The coefficients of $\sin\theta$, $\cos\theta$ and 1 are presented, for clarity, in a tabular form in Table 1. Thus, we now have potential energy of constant and spring loads expressed as functions of configuration variable $\theta$.

**2.2 Invariance of Potential Energy With Respect to the Configuration Variable**

*2.2.1 Trivial Conditions.* The potential energy of the spring on the lever can have constant potential energy only under trivial conditions: (1) the spring stiffness is zero $(k = 0)$, (2) the anchor point on the lever is at the hinge point $(\boldsymbol{a} = 0)$, and (3) the anchor point on the global frame is at the hinge point $(\boldsymbol{b} = \boldsymbol{r})$. Similar trivial conditions for the constant loads are (1) the load is zero $(\boldsymbol{f} = \boldsymbol{0})$ and (2) the load acts at the pivot point $(\boldsymbol{p} = \boldsymbol{0})$. It is only under these trivial conditions that the coefficients of $\cos\theta$ and $\sin\theta$ become zero in Table 1.

*2.2.2 The Discovery of Lucien LaCoste.* Even though a nontrivial spring and a nontrivial constant load cannot be individually in static balance, they together can be, as demonstrated in Fig. 4. This was first recognized by Lucien LaCoste (see Ref. [1]) in the context of having a pendulum of infinite period. Figure 4 shows a lever under the action of a weight $W$ that is balanced by a zero-

**Table 1 Potential energy of the weight and the zero-free-length component of the spring acting on the lever is a linear combination of cos $\theta$, sin $\theta$, and 1.**

| | Coefficients | |
|---|---|---|
| Basis | Weight | Zero-free-length component of spring load |
| cos $\theta$ | $-\boldsymbol{f}^T\boldsymbol{p} = -(f_y p_y + f_x p_x)$ | $k(\boldsymbol{r}-\boldsymbol{b})^T\boldsymbol{a} = k(a_y r_y + a_x r_x - a_y b_y - a_x b_x)$ |
| sin $\theta$ | $-\boldsymbol{f}^T\boldsymbol{R}\left(\frac{\pi}{2}\right)\boldsymbol{p} = (f_x p_y - f_y p_x)$ | $k(\boldsymbol{r}-\boldsymbol{b})^T\boldsymbol{R}\left(\frac{\pi}{2}\right)\boldsymbol{a} = k(a_x r_y - a_y r_x - a_x b_y + a_y b_x)$ |
| 1 | $-\boldsymbol{f}^T\boldsymbol{r} = -f_y r_y - f_x r_x$ | $+\frac{k}{2}\left(\boldsymbol{r}^T\boldsymbol{r} + \boldsymbol{a}^T\boldsymbol{a} + \boldsymbol{b}^T\boldsymbol{b} - 2\boldsymbol{r}^T\boldsymbol{b}\right) = +\frac{k}{2}(r_y^2 - 2b_y r_y + r_x^2 - 2b_x r_x + b_y^2 + b_x^2 + a_y^2 + a_x^2)$ |

free-length spring of spring constant $k$ anchored above the pivot of the lever at a height of $h$. As shown in the figure, under the condition $W = kh$, the potential energy is invariant with respect to configuration variable $\theta$.

*2.2.3 Several Zero-Free-Length Springs and Constant Loads.* The balancing condition $W = kh$ of the example in Fig. 4 will now be generalized to a lever under several constant loads and zero-free-length spring loads. Since several loads are now being considered, let both constant loads and zero-free-length spring loads be ordered to allow indexing. The notation $\boldsymbol{a}_i$, $\boldsymbol{b}_i$, $k_i$, has the same meaning as $\boldsymbol{a}$, $\boldsymbol{b}$, and $k$ in Fig. 3 other than that it corresponds to $i$th spring. $\boldsymbol{f}_i$ and $\boldsymbol{p}_i$ also have similar meaning. Further, let the number of constant loads be $n_c$ and the number of zero-free-length spring loads be $n_s$.

Since the potential energy of each of the constant loads and the zero-free-length spring loads are a linear combination of cos $\theta$, sin $\theta$ and 1, their net potential energy is also a linear combination of cos $\theta$, sin $\theta$ and 1. Further, since cos $\theta$ and sin $\theta$ and 1 are linearly independent functions of $\theta$, their linear combination is a constant if and only if the coefficients of nonconstant functions, i.e., cos $\theta$ and sin $\theta$ are zero. Writing, with the help of Table 1, the coefficients of cos $\theta$ and sin $\theta$ of the net potential energy of all the loads and equating them to zero lead to the following equations:

$$-\sum_{i=1}^{n_c}\left(f_{y,i}p_{y,i} + f_{x,i}p_{x,i}\right) + \sum_{i=1}^{n_s} k_i\left(a_{y,i}r_y + a_{x,i}r_x - a_{y,i}b_{y,i} - a_{x,i}b_{x,i}\right) = 0 \quad (10)$$

$$\sum_{i=1}^{n_c}\left(f_{x,i}p_{y,i} - f_{y,i}p_{x,i}\right) + \sum_{i=1}^{n_s} k_i\left(a_{x,i}r_y - a_{y,i}r_x - a_{x,i}b_{y,i} + a_{y,i}b_{x,i}\right) = 0 \quad (11)$$

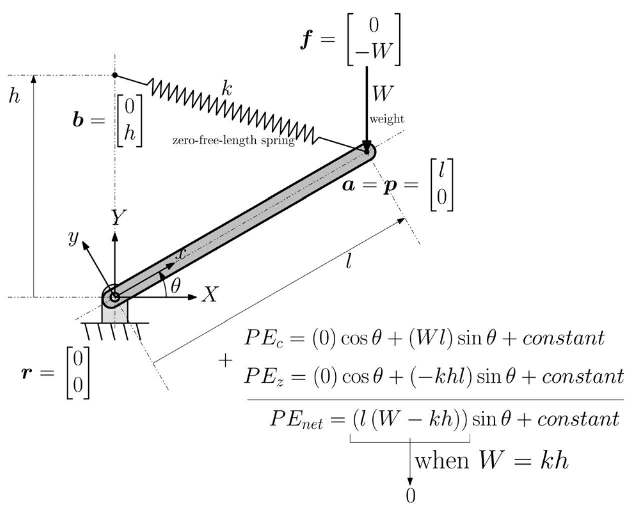


**Fig. 4 Static balancing of a weight by a spring**

which are the conditions for constant potential energy (or static balance) of several constant and zero-free-length spring loads on a lever. These conditions are applicable to all the three categories of Fig. 1. Further, by choosing appropriate load parameters, it is possible to satisfy the conditions *in practice*, as was the case in the example of Fig. 4.

*2.2.4 Normal Positive-Free-Length Springs.* As far as normally available positive-free-length springs are concerned, the square root term in Eq. (8) poses a severe restriction on static balancing, as explained in detail in Appendix A. Hence, for the remainder of this paper, all the spring loads are of zero-free-length with the understanding that a positive-free-length spring can be brought into the ambit of zero-free-length by combining it with an appropriate negative-free-length spring.

Our next aim is to derive a set of conditions for the static balance of a revolute-jointed multibody linkage loaded by constant loads and zero-free-length spring loads. Before that, it is useful to consider the static balance of a single rigid body moving freely in a plane.

## 3 Balancing of a Rigid Body in a Plane

Consider the rigid body shown in Fig. 3. An appropriate set of configuration variables for the body is $\{\boldsymbol{r},\theta\}$. It may be noted that $\boldsymbol{r}$ in Fig. 5, in contrast to Fig. 3, is an independent *variable* because the body is free to move in the plane.

The loads on the body are a set of zero-free-length spring loads and constant loads, and both sets of loads are exerted by the global frame of reference as shown in Fig. 5. The notations $n_c$, $n_s$, $\boldsymbol{a}_i$, $\boldsymbol{b}_i$, $k_i$, $\boldsymbol{f}_i$, and $\boldsymbol{p}_i$ have the same meaning as in Sec. 2. The potential energy of the loads is also the same as in Sec. 2 except that $r_x$ and $r_y$ are now independent variables. In Table 1 of Sec. 2, when linearly independent functions of $\{\boldsymbol{r},\theta\}$ are pulled out as basis functions, Table 2 is obtained. As is evident from Table 2, the potential energy of the loads is now a linear combination of the following basis functions: cos $\theta$, sin $\theta$, $r_x$ cos $\theta$, $r_y$ cos $\theta$, $r_x$ sin $\theta$, $r_y$ sin $\theta$, $r_x^2$, $r_y^2$, $r_x$, $r_y$, and 1.

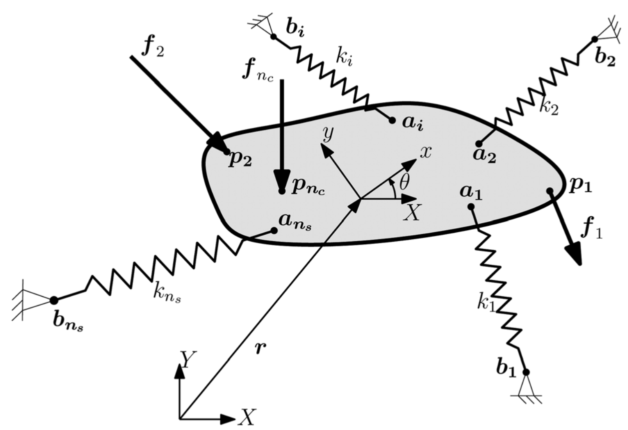


**Fig. 5 A body that is free to move in a plane**

**Table 2 Potential energy of weight and spring acting on a link moving in a plane.**

| | Coefficients of the basis | | |
|---|---|---|---|
| Basis | Weight | Spring load | Generalized potential (see Eq. (15) |
| $\cos\theta$ | $-(f_y p_y + f_x p_x)$ | $-k(a_y b_y + a_x b_x)$ | $(q_y w_y + q_x w_x)$ |
| $\sin\theta$ | $+(f_x p_y - f_y p_x)$ | $-k(a_x b_y - a_y b_x)$ | $(q_x w_y - q_y w_x)$ |
| $r_x \cos\theta$ | 0 | $ka_x$ | $v_x$ |
| $r_y \cos\theta$ | 0 | $ka_y$ | $v_y$ |
| $r_x \sin\theta$ | 0 | $-ka_y$ | $-v_y$ |
| $r_y \sin\theta$ | 0 | $ka_x$ | $v_x$ |
| $r_x^2$ | 0 | $\frac{k}{2}$ | $\kappa$ |
| $r_y^2$ | 0 | $\frac{k}{2}$ | $\kappa$ |
| $r_x$ | $-f_x$ | $-kb_x$ | $u_x$ |
| $r_y$ | $-f_y$ | $-kb_y$ | $u_y$ |
| 1 | 0 | $+\frac{k}{2}(a_x^2 + a_y^2 + b_x^2 + b_y^2)$ | $c$ |

The net potential energy of $n_c$ constant loads and $n_s$ spring loads is also a linear combinations of the same basis functions. Furthermore, $\cos\theta$, $\sin\theta$, $r_x\cos\theta$, $r_y\cos\theta$, $r_x\sin\theta$, $r_y\sin\theta$, $r_x^2$, $r_y^2$, $r_x$, $r_y$, and 1 are linearly independent functions of $\{\boldsymbol{r},\theta\}$. Hence, from a reasoning similar to the one in Sec. 2, for the net potential energy to be independent of the configuration variables, the coefficients of all the basis functions other than 1 have to be zero. However, it is not practical to make the coefficients of all these functions as zeros because of the following reasons:

- There are only gravity loads: Gravity is the most important practically seen instance of a constant load. When all the constant loads are gravity loads, $\boldsymbol{f}_i = m_i \boldsymbol{g}_i$, where $m_i$ is the mass and $\boldsymbol{g}$ is the acceleration due to gravity. Further, the coefficient of $r_x$ and $r_y$ become $\left(-g_x \sum_{i=1}^{n_g} m_i\right)$ and $\left(-g_y \sum_{i=1}^{n_g} m_i\right)$. Since $m_i > 0$, $\forall i$, $\sum_{i=1}^{n_g} m_i > 0$. Also, since the acceleration due to gravity is nonzero, both $g_x$ and $g_y$ cannot be zero. Hence, the coefficients of both $r_x$ and $r_y$ cannot be zero.
- There are zero-free-length spring loads, possibly with gravity loads: In this case, the coefficients of both $r_x^2$ and $r_y^2$ are $\sum_{i=1}^{n_s} k_i$. Since the spring constants of all the springs considered here are positive, $(k_i > 0, \forall i)$, $\sum_{i=1}^{n_s} k_i$ cannot be zero. Hence, the coefficients of $r_x^2$ and $r_y^2$ cannot be zero.

However, as shown in Appendix B.1, there is no such practical difficulty in making the coefficients of all $\theta$-dependent functions, i.e., $\cos\theta$, $\sin\theta$, $r_x\cos\theta$, $r_y\cos\theta$, $r_x\sin\theta$, and $r_y\sin\theta$ as zero. Setting $\theta$-dependent terms to zero amounts to the following set of independent constraints:

$$-\sum_{i=1}^{n_c}\left((f_{y,i}p_{y,i} + f_{x,i}p_{x,i})\right) - \sum_{i=1}^{n_s}\left(k_i(a_{y,i}b_{y,i} + a_{x,i}b_{x,i})\right) = 0 \quad (12)$$

$$+\sum_{i=1}^{n_c}\left((f_{x,i}p_{y,i} - f_{y,i}p_{x,i})\right) - \sum_{i=1}^{n_s}\left(k_i(a_{x,i}b_{y,i} - a_{y,i}b_{x,i})\right) = 0 \quad (13)$$

$$\sum_{i=1}^{n_s}(k_i \boldsymbol{a}_i) = \boldsymbol{0} \quad (14)$$

It is shown in Appendix B.1 that if these constraints are not satisfied by the loads, then by adding not more than two zero-free-length springs, these constraints can be satisfied. A numerical example to demonstrate the same is given in Fig. 6.

Inspite of being able to make the potential energy of the loads on the link independent of $\theta$, the dependency on $\boldsymbol{r}$ still remains. In Sec. 4, we show that if the body is joined to an appropriate linkage, then by adding extra loads to other parts of the linkage, the $\boldsymbol{r}$-dependent terms of the potential energy can be balance out.

Before we proceed to Sec. 4, it may be noted that the potential energy of a constant load or a zero-free-length spring load falls under the following general form:

$$\Phi = \boldsymbol{r}^T\boldsymbol{u} + \kappa\boldsymbol{r}^T\boldsymbol{r} + \boldsymbol{r}^T\boldsymbol{R}(\theta)\boldsymbol{v} + \boldsymbol{w}^T\boldsymbol{R}(\theta)\boldsymbol{q} + c \quad (15)$$

where $\theta$ and $\boldsymbol{r}$ are the configuration variables of the rigid body on which the load acts. In the case of constant loads, by comparing Eq. (1) with Eq. (15), we have

$$\boldsymbol{u} = -\boldsymbol{f}, \quad \kappa = 0, \quad \boldsymbol{v} = \boldsymbol{0}, \quad \boldsymbol{w} = -\boldsymbol{f}, \quad \boldsymbol{q} = \boldsymbol{p}, \quad \text{and} \quad \boldsymbol{c} = 0 \quad (16)$$

and in the case of zero-free-length spring loads, by comparing Eqs. (6) and (15), we have

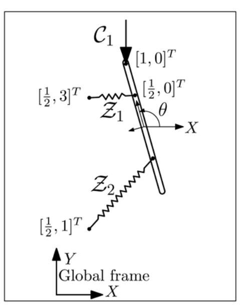


| Spring Loads | $\boldsymbol{a}$ | $\boldsymbol{b}$ | $k$ |
|---|---|---|---|
| $\mathcal{Z}_1$ | $[\frac{1}{2},0]^T$ | $[\frac{1}{2},3]^T$ | 1 |
| $\mathcal{Z}_2$ | $[-\frac{1}{2},0]^T$ | $[\frac{1}{2},1]^T$ | 1 |

| Constant Loads | $\boldsymbol{p}$ | $\boldsymbol{f}$ |
|---|---|---|
| $\mathcal{C}_1$ | $[1,0]^T$ | $[0,-1]^T$ |

| $-k\boldsymbol{b}^T\boldsymbol{a}$ | $-k\boldsymbol{b}^T\boldsymbol{R}\left(\frac{pi}{2}\right)\boldsymbol{a}$ | $k\boldsymbol{a}$ |
|---|---|---|
| $\frac{1}{4}$ | $\frac{3}{2}$ | $[\frac{1}{2},0]^T$ |
| $-\frac{1}{4}$ | $-\frac{1}{2}$ | $[-\frac{1}{2},0]^T$ |
| $-\boldsymbol{f}^T\boldsymbol{p}$ | $-\boldsymbol{f}^T\boldsymbol{R}\left(\frac{pi}{2}\right)\boldsymbol{p}$ | |
| 0 | $-1$ | |

**Fig. 6 A rigid body moving freely in a plane under a constant load is made to have $\theta$-independent potential energy by addition of two zero-free-length springs**

$$\boldsymbol{u} = -k\boldsymbol{b}, \quad \kappa = \frac{k}{2}, \quad \boldsymbol{v} = k\boldsymbol{a}, \quad \boldsymbol{w} = -\boldsymbol{b},$$

$$\boldsymbol{q} = k\boldsymbol{a}, \text{ and } \quad c = \frac{k}{2}\left(\boldsymbol{b}^T\boldsymbol{b} + \boldsymbol{a}^T\boldsymbol{a}\right) \tag{17}$$

Later in the paper, we encounter potential energy functions that are of the form given in Eq. (15), but they cannot be attributed to zero-free-length spring loads or constant loads *acting on the body*. Hence, there is a need to generalize constraints (10)–(14) to the form given in Eq. (15). Such a generalization is possible because as can be seen in the last column of Table 2, the potential given in Eq. (15) is a linear combination of the basis functions given in Table 2 just as in the case of constant and zero-free-length spring loads. The following proposition states the generalization.

Proposition 3.1. If there are $n$ functions of the form

$$\Phi_i = \boldsymbol{r}^T\boldsymbol{u}_i + \kappa_i\boldsymbol{r}^T\boldsymbol{r} + \boldsymbol{r}^T\boldsymbol{R}(\theta)\boldsymbol{v}_i + \boldsymbol{w}_i^T\boldsymbol{R}(\theta)\boldsymbol{q}_i + c_i, \quad i = 1\cdots n \tag{18}$$

with $\boldsymbol{r}$ and $\theta$ as the variables, then $\sum_{i=1}^{n}\Phi_i$ is independent of $\theta$ if and only if the following constraints are satisfied:

$$\sum_{i=1}^{n}\left(q_{y,i}w_{y,i} + q_{x,i}w_{x,i}\right) = 0 \tag{19}$$

$$\sum_{i=1}^{n}\left(q_{x,i}w_{y,i} - q_{y,i}w_{x,i}\right) = 0 \tag{20}$$

$$\sum_{i=1}^{n}\boldsymbol{v}_i = \boldsymbol{0} \tag{21}$$

When these constraints are satisfied, $\sum_{i=1}^{n}\Phi_i$ depends only on $\boldsymbol{r}$ in the following form:

$$\sum_{i=1}^{n}\Phi_i = \sum_{i=1}^{n}\left(\boldsymbol{r}^T\boldsymbol{u}_i + \kappa_i\boldsymbol{r}^T\boldsymbol{r} + c_i\right) = \left(\boldsymbol{r}^T\right)\sum_{i=1}^{n}\boldsymbol{u}_i + \left(\boldsymbol{r}^T\boldsymbol{r}\right)\sum_{i=1}^{n}\kappa_i + \sum_{i=1}^{n}c_i \tag{22}$$

Furthermore, if $\boldsymbol{r}$ happens to be a constant (as in a lever) with only $\theta$ being the variable, then $\sum_{i=1}^{n}\Phi_i$ is independent of $\theta$ (and hence a constant) if and only if the following constraints are satisfied:

$$\sum_{i=1}^{n}\left(v_{y,i}r_y + v_{x,i}r_x + q_{y,i}w_{y,i} + q_{x,i}w_{x,i}\right) = 0 \tag{23}$$

$$\sum_{i=1}^{n}\left(v_{x,i}r_y - v_{y,i}r_x + q_{x,i}w_{y,i} - q_{y,i}w_{x,i}\right) = 0 \tag{24}$$

*Proof*. The proof is along the same lines as the derivation of Eqs. (10)–(14).

It may be noted that inspite of considering a general form of potential in Eq. (18), the inability to make the net potential energy independent of $\boldsymbol{r}$ remains because of the following reason. In all the cases that we consider next, $\boldsymbol{\kappa}_i \geq 0$ and $\boldsymbol{\kappa}_i > 0$ for atleast one value of $i$. Hence, the $\boldsymbol{r}$-dependent term, $\sum_{i=1}^{n}\boldsymbol{\kappa}_i\boldsymbol{r}^T\boldsymbol{r}$, cannot be zero in the expression for $\sum_{i=1}^{n}\Phi_i$.

## 4 New Static Balancing Techniques for Revolute-Jointed Linkages

If there is a single rigid body with loads exerted by a reference frame, then the net potential energy of the loads depends on the configuration of the body with respect to the reference frame. If there are several such bodies, then the net potential energy of all the loads *on all the bodies* depends on the configuration of *all the bodies*. This dependency on the configuration of *all the bodies* can be reduced to that of a *single body* provided the bodies are connected by revolute joints (to begin with, say, in a serial or a tree-structured manner) and the loads are zero-free-length spring loads and constant loads. If this single body is the reference frame itself, then the net potential energy is a constant (implying static balance) since the configuration of the reference frame with respect to itself is always fixed. This result follows as a consequence of the proposition that is presented next.

### 4.1 The Potential Energy of Loads on a Body Transformed as a Function of Another Body.

We are now considering several rigid bodies, each of them with its own $\boldsymbol{r}$, $\theta$, $n_c$, $n_s$, $\boldsymbol{a}_i$, $\boldsymbol{b}_i$, $k_i$, $\boldsymbol{p}_i$, etc. To distinguish these quantities belonging to different rigid bodies, we number the rigid bodies and put the number as a superscript to these symbols. Hence $\boldsymbol{r}$, $\theta$, $n_c$, $n_s$, $\boldsymbol{a}_i$, $\boldsymbol{b}_i$, $k_i$, $\boldsymbol{p}_i$, and $\boldsymbol{f}_i$ of body $j$ are now represented as $\boldsymbol{r}^j$, $\theta^j$, $n_c^j$, $n_s^j$, $\boldsymbol{a}_i^j$, $\boldsymbol{b}_i^j$, $k_i^j$, $\boldsymbol{p}_i^j$, etc.

Proposition 4.1. The net sum of a set of functions of the configuration variables of a body $l$ in the form given in Eq. (15), i.e.

$$\Phi_i^l = \boldsymbol{r}^{l^T}\boldsymbol{u}_i^l + \boldsymbol{\kappa}_i^l\boldsymbol{r}^{l^T}\boldsymbol{r}^l + \boldsymbol{r}^{l^T}\boldsymbol{R}\left(\theta^l\right)\boldsymbol{v}_i^l + \boldsymbol{w}_i^{l^T}\boldsymbol{R}\left(\theta^l\right)\boldsymbol{q}_i^l + c_i^l, \quad i = 1\cdots n^l \tag{25}$$

can be expressed as a function of the same form but of body $j$, i.e.

$$\sum_{i=1}^{n^l}\Phi_i^l = \Phi_i^j = \boldsymbol{r}^{j^T}\boldsymbol{u}_i^j + \kappa_i^j\boldsymbol{r}^{j^T}\boldsymbol{r}^j + \boldsymbol{r}^{j^T}\boldsymbol{R}\left(\theta^j\right)\boldsymbol{v}_i^j + \boldsymbol{w}_i^{j^T}\boldsymbol{R}\left(\theta^j\right)\boldsymbol{q}_i^l + c_i^j \tag{26}$$

provided the following conditions are satisfied:

Condition 1: There is a point that is rigidly fixed to both body $l$ and body $j$. Such a point is called as a common point of bodies $l$ and $j$.
Condition 2: The origin of the local coordinate frame of body $l$ is at the common point.
Condition 3: The sum of the set of functions of body $l$ is dependent only on $\boldsymbol{r}$ in the form given in Eq. (22).

*Proof*. Let the local coordinate of the common point required by condition 1 in body $l$ be $\boldsymbol{s}_j^l$ and in body $j$ be $\boldsymbol{s}_l^j$. The commonality of the point can be written as follows:

$$\boldsymbol{r}^l + \boldsymbol{R}\left(\theta^l\right)\boldsymbol{s}_j^l = \boldsymbol{r}^j + \boldsymbol{R}\left(\theta^j\right)\boldsymbol{s}_l^j \tag{27}$$

Condition 2 implies that $\boldsymbol{s}_j^l = \boldsymbol{0}$. Substituting $\boldsymbol{s}_j^l = \boldsymbol{0}$ into Eq. (27) leads to

$$\boldsymbol{r}^l = \boldsymbol{r}^j + \boldsymbol{R}\left(\theta^j\right)\boldsymbol{s}_l^j \tag{28}$$

Condition 3 implies that the sum of the set of functions of body $l$ can be written as

$$\sum_{i=1}^{n^l}\Phi_i^l = \boldsymbol{r}^{l^T}\sum_{i=1}^{n^l}\boldsymbol{u}_i^l + \left(\boldsymbol{r}^{l^T}\boldsymbol{r}^l\right)\sum_{i=1}^{n^l}\kappa_i^l \tag{29}$$

The constant term is omitted in Eq. (29) since it is inconsequential for the discussion.

Substitution of $\boldsymbol{r}^l$ from Eq. (28) into Eq. (29) and simplification using the fact that $\boldsymbol{R}^T(\theta)\boldsymbol{R}(\theta)$ is identity lead to the following expression for $\sum_{i=1}^{n^l}\Phi_i^l$:

$$\mathbf{r}^{j^T}\overbrace{\left(\sum_{i=1}^{n^l}\mathbf{u}_i^l\right)}^{\mathbf{u}_i^j}+\mathbf{r}^{j^T}\mathbf{r}^j\overbrace{\left(\sum_{i=1}^{n^l}\kappa_i^l\right)}^{\kappa_i^j}+\mathbf{r}^{j^T}\mathbf{R}(\theta^j)\overbrace{\left(2\mathbf{s}_l^j\sum_{i=1}^{n^l}\kappa_i^l\right)}^{\mathbf{v}_i^j}$$
$$+\overbrace{\left(\sum_{i=1}^{n^l}\mathbf{u}_i^l\right)^T}^{\mathbf{w}_i^{j^T}}\mathbf{R}(\theta^j)\overbrace{\left(\mathbf{s}_l^j\right)}^{\mathbf{q}_i^j}=\sum_{i=1}^{n^l}\Phi_i^l=\Phi_i^j \qquad (30)$$

Again, the constant term is omitted in Eq. (30). It may be readily recognized that the sum of the set of functions on body $l$, $\sum_{i=1}^{n^l}\Phi_i^l$, as seen in Eq. (30) is indeed of the form given in Eq. (26).

**4.2 Proposition 4.1 as the Recursive Relation of an Iterative Static Balancing Algorithm.** We now show that Proposition 4.1 can be treated as a recursive relation that can be incorporated into an iterative procedure to achieve static balance of a linkage. For the purpose of this section, we restrict the linkage on which the iterative procedure can be applied to have the following features:

(1) The linkage should be tree-structured (i.e., no closed loops). This feature is necessary since a recursive relation requires a tree-structure to propagate.
(2) All the joints of the tree-structure should be revolute joints. This feature is necessary to satisfy condition 1 of Proposition 4.1.
(3) We want all the loads to have potential energy functions of the form given in Eq. (25) of Proposition 4.1. While we know that zero-free-length springs and constant loads do have this form (see Eqs. (16) and (17)), the fact that there are several bodies involved requires attention. The configuration variables ($\mathbf{r}^l$,$\theta^l$) of different bodies (i.e., of different $l$) should be with respect to a common global frame of reference. Hence constant loads on all the bodies should be constant with respect to a common global reference frame and any zero-free-length spring should have its one anchor point on the same common global frame while the other anchor point can be on any of the bodies constituting the linkage.
(4) The common reference frame should be one of the bodies of the linkage, i.e., it should join to body/bodies of the linkage by revolute joint/joints.

*4.2.1 The Iterative Static Balancing Algorithm.* We now present the iterative algorithm and prove that it leads to static balance.

*Preparatory Steps*

(1) Assign the reference body as the root node of the tree-structure (bodies are represented as nodes and joints as lines joining the nodes). With this assignment, for every link/body other than the root, there is a parent body. Further, every link other than a terminal link has one or more children.
(2) Choose a local frame of reference on every link to coincide with the center of revolute joint between the link and its parent. For every link $k$, $\mathbf{r}^k$ and $\theta^k$ decide the configuration of its local frame with respect the frame of the root.
(3) Give this tree-structure with the given constant and zero-free-length spring loads (together referred to as original loads) as an input to the following iterative procedure.

*Iterative Procedure.* Entry condition: If the tree-structure contains only the root node, then exit from the iterative procedure. Otherwise, proceed to step 1.

Step 1: Any terminal node $l$, has associated with it the following three kinds of potential energy functions: (1) due to original loads on body $l$, (2) due to association that happened in step 3 of previous iterations, and (3) additional loads on body $l$. Let the number of such functions be represented by $n_o^l$, $n_c^l$, $n_a^l$, respectively. The first two kinds of functions are known from the given problem and previous iterations, respectively, and the task in this step is to find the additional loads so that

Case (a): Equations (19)–(21) are satisfied if $l$ is not a child (i.e., not first generation descendant) of the root.

Case (b): Equations (23)–(24) are satisfied if $l$ is a child of the root. Note that in this case $\mathbf{r}^l$ is a constant because of the way local frame is chosen in the preparatory steps.

This task makes sense only if the all kinds of potential energy functions fall under the form of Eq. (15) with ($\mathbf{r}$, $\theta$) being ($\mathbf{r}^l$, $\theta^l$). The first and the third kind of potential energy functions do fall under the form because of the kind of loads we are restricting to (see Eqs. (16) and (17)). The second kind of potential energy functions conform to the form because of step 2 which is a direct consequence of Proposition 4.1. *The critical role of Proposition 4.1 in enabling this iterative procedure may be noted.* Further, Appendix B.2 asserts that the task of this step is always feasible. It may be noted that there are several set of additional loads that satisfy these equations. This nonuniqueness calls for discretion of the designer in choosing a suitable set of additional loads.

Step 2: In case (a), express $\sum_{i=1}^{n_o^l+n_c^l+n_a^l}\Phi_i^l$ in the form given in Eq. (15) where $\mathbf{r}$ and $\theta$ are the configuration variables of the *parent* of node $l$. This is possible since condition 1 (because of revolute joint), condition 2 (because of preparatory steps) and condition 3 (because of step 1) of Proposition 4.1 are satisfied. In case (b), recognize that $\sum_{i=1}^{n_o^l+n_c^l+n_a^l}\Phi_i^l$ is a constant as per Proposition 3.1.

Step 3: Associate $\sum_{i=1}^{n_o^l+n_c^l+n_a^l}\Phi_i^l$ with the parent link of $l$ and for energy conservation, disassociate $\Phi_i^l$, $i=1\cdots n_o^l+n_c^l+n_a^l$ from node $l$. Because of this association, $n_c^{\mathfrak{p}(l)}$ ($\mathfrak{p}(l)$ denotes parent node of $l$, and $n_c^k$ denotes the number of potential energy functions associated with node $k$ *so far* at step 3) gets incremented by one and the associated function can be written as

$$\Phi_{n_c}^{\mathfrak{p}(l)}=\sum_{i=1}^{n_o^l+n_c^l+n_a^l}\Phi_i^l \qquad (31)$$

Step 4: With all potential energy functions "robed" from node $l$ to its parent, delete this *terminal* node $l$.

Iterator: Once steps 1–4 are completed, a new trimmed tree-structure results where the parents of the nodes deleted in step 4 has additional potential energy functions associated with them. Follow this iterative procedure again with this trimmed tree-structure as the input.

With every iteration, the tree-structure shrinks and it eventually gets reduced to the single root node. Any of the $n_c^0$ potential energy functions (of the second kind) associated with this reduced root is from one of the children of the root. As per step 1, this association is through case (b). Any function associated through case (b) is a constant as recognized in step 2. Thus, the sum of these $n_c^0$ potential energy functions is also constant. Further, the sum of these $n_c^0$ potential energy functions is actually the sum potential energy of original loads and additional loads on all the descendants of the root. This can be verified by recursive substitution in Eq. (31) as exemplified in Eq. (32). Therefore, the original loads are in static balance with the additional loads.

Illustration of the algorithm on a 4R linkage under constant loads: Figure 7 shows a 4R linkage where four revolute joints connect the ground and four other bodies serially. The ground exerts constant gravitational force on each of the four bodies. Hence we take the ground as the root and number the bodies accordingly as shown in Fig. 7(*b*). The local frame of reference are located on each of the bodies as per the preparatory step 2. The constant loads on bodies 1–4 are represented as $\mathcal{C}_1^1$, $\mathcal{C}_1^2$, $\mathcal{C}_1^3$, and $\mathcal{C}_1^4$, respectively. Their details (point of action $\mathbf{p}$ and force vector $\mathbf{f}$) are presented in item number 1, 4, 7, and 10 of the table in Fig. 7.

Now we give the tree-structure to the iterative procedure. The terminal node of the tree is 4. There is a potential energy function associated with the node due to $\mathcal{C}_1^4$ which is represented as

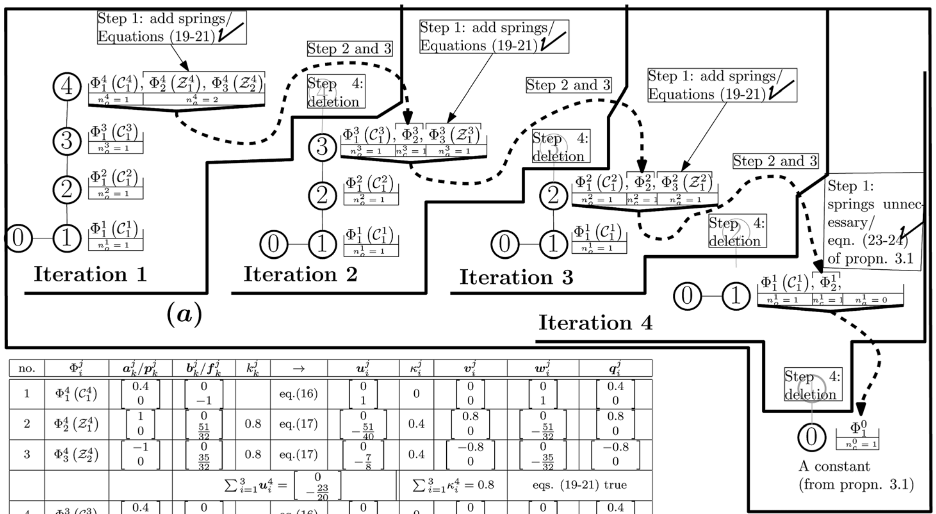


| no. | $\Phi_i^j$ | $\boldsymbol{a}_k^j/\boldsymbol{p}_k^j$ | $\boldsymbol{b}_k^j/\boldsymbol{f}_k^j$ | $k_k^j$ | $\rightarrow$ | $\boldsymbol{u}_i^j$ | $\kappa_i^j$ | $\boldsymbol{v}_i^j$ | $\boldsymbol{w}_i^j$ | $\boldsymbol{q}_i^j$ |
|---|---|---|---|---|---|---|---|---|---|---|
| 1 | $\Phi_1^4(\mathcal{C}_1^4)$ | $\begin{bmatrix}0.4\\0\end{bmatrix}$ | $\begin{bmatrix}0\\-1\end{bmatrix}$ | | eq.(16) | $\begin{bmatrix}0\\1\end{bmatrix}$ | 0 | $\begin{bmatrix}0\\0\end{bmatrix}$ | $\begin{bmatrix}0\\1\end{bmatrix}$ | $\begin{bmatrix}0.4\\0\end{bmatrix}$ |
| 2 | $\Phi_2^4(\mathcal{Z}_1^4)$ | $\begin{bmatrix}1\\0\end{bmatrix}$ | $\begin{bmatrix}0\\\frac{51}{32}\end{bmatrix}$ | 0.8 | eq.(17) | $\begin{bmatrix}0\\-\frac{51}{40}\end{bmatrix}$ | 0.4 | $\begin{bmatrix}0.8\\0\end{bmatrix}$ | $\begin{bmatrix}0\\-\frac{51}{32}\end{bmatrix}$ | $\begin{bmatrix}0.8\\0\end{bmatrix}$ |
| 3 | $\Phi_3^4(\mathcal{Z}_2^4)$ | $\begin{bmatrix}-1\\0\end{bmatrix}$ | $\begin{bmatrix}0\\\frac{35}{32}\end{bmatrix}$ | 0.8 | eq.(17) | $\begin{bmatrix}0\\-\frac{7}{8}\end{bmatrix}$ | 0.4 | $\begin{bmatrix}-0.8\\0\end{bmatrix}$ | $\begin{bmatrix}0\\-\frac{35}{32}\end{bmatrix}$ | $\begin{bmatrix}-0.8\\0\end{bmatrix}$ |
| | | | $\sum_{i=1}^{3}\boldsymbol{u}_i^4 = \begin{bmatrix}0\\-\frac{23}{20}\end{bmatrix}$ | | | | $\sum_{i=1}^{3}\kappa_i^4 = 0.8$ | | eqs. (19-21) true | |
| 4 | $\Phi_1^3(\mathcal{C}_1^3)$ | $\begin{bmatrix}0.4\\0\end{bmatrix}$ | $\begin{bmatrix}0\\-1\end{bmatrix}$ | | eq.(16) | $\begin{bmatrix}0\\1\end{bmatrix}$ | 0 | $\begin{bmatrix}0\\0\end{bmatrix}$ | $\begin{bmatrix}0\\1\end{bmatrix}$ | $\begin{bmatrix}0.4\\0\end{bmatrix}$ |
| 5 | $\Phi_2^3$ | $\boldsymbol{s}_4^3 =$ | $\begin{bmatrix}1\\0\end{bmatrix}$ | | eq.(30) | $\begin{bmatrix}0\\-\frac{23}{20}\end{bmatrix}$ | 0.8 | $\begin{bmatrix}1.6\\0\end{bmatrix}$ | $\begin{bmatrix}0\\-\frac{23}{20}\end{bmatrix}$ | $\begin{bmatrix}1\\0\end{bmatrix}$ |
| 6 | $\Phi_3^3(\mathcal{Z}_1^3)$ | $\begin{bmatrix}-1\\0\end{bmatrix}$ | $\begin{bmatrix}0\\\frac{15}{32}\end{bmatrix}$ | 1.6 | eq.(17) | $\begin{bmatrix}0\\-\frac{3}{4}\end{bmatrix}$ | 0.8 | $\begin{bmatrix}-1.6\\0\end{bmatrix}$ | $\begin{bmatrix}0\\-\frac{15}{32}\end{bmatrix}$ | $\begin{bmatrix}-1.6\\0\end{bmatrix}$ |
| | | | $\sum_{i=1}^{3}\boldsymbol{u}_i^3 = \begin{bmatrix}0\\-\frac{9}{10}\end{bmatrix}$ | | | | $\sum_{i=1}^{3}\kappa_i^3 = 1.6$ | | eqs. (19-21) true | |
| 7 | $\Phi_1^2(\mathcal{C}_1^2)$ | $\begin{bmatrix}0.4\\0\end{bmatrix}$ | $\begin{bmatrix}0\\-1\end{bmatrix}$ | | eq.(16) | $\begin{bmatrix}0\\1\end{bmatrix}$ | 0 | $\begin{bmatrix}0\\0\end{bmatrix}$ | $\begin{bmatrix}0\\1\end{bmatrix}$ | $\begin{bmatrix}0.4\\0\end{bmatrix}$ |
| 8 | $\Phi_2^2$ | $\boldsymbol{s}_3^2 =$ | $\begin{bmatrix}1\\0\end{bmatrix}$ | | eq.(30) | $\begin{bmatrix}0\\-\frac{9}{10}\end{bmatrix}$ | 1.6 | $\begin{bmatrix}3.2\\0\end{bmatrix}$ | $\begin{bmatrix}0\\-\frac{9}{10}\end{bmatrix}$ | $\begin{bmatrix}1\\0\end{bmatrix}$ |
| 9 | $\Phi_3^2(\mathcal{Z}_1^2)$ | $\begin{bmatrix}-1\\0\end{bmatrix}$ | $\begin{bmatrix}0\\\frac{5}{32}\end{bmatrix}$ | 3.2 | eq.(17) | $\begin{bmatrix}0\\-\frac{1}{2}\end{bmatrix}$ | 1.6 | $\begin{bmatrix}-3.2\\0\end{bmatrix}$ | $\begin{bmatrix}0\\-\frac{5}{32}\end{bmatrix}$ | $\begin{bmatrix}-3.2\\0\end{bmatrix}$ |
| | | | $\sum_{i=1}^{3}\boldsymbol{u}_i^2 = \begin{bmatrix}0\\-\frac{2}{5}\end{bmatrix}$ | | | | $\sum_{i=1}^{3}\kappa_i^2 = 3.2$ | | eqs. (19-21) true | |
| 10 | $\Phi_1^1(\mathcal{C}_1^1)$ | $\begin{bmatrix}0.4\\0\end{bmatrix}$ | $\begin{bmatrix}0\\-1\end{bmatrix}$ | | eq.(16) | $\begin{bmatrix}0\\1\end{bmatrix}$ | 0 | $\begin{bmatrix}0\\0\end{bmatrix}$ | $\begin{bmatrix}0\\1\end{bmatrix}$ | $\begin{bmatrix}0.4\\0\end{bmatrix}$ |
| 11 | $\Phi_2^1$ | $\boldsymbol{s}_2^1 =$ | $\begin{bmatrix}1\\0\end{bmatrix}$ | | eq.(30) | $\begin{bmatrix}0\\-\frac{2}{5}\end{bmatrix}$ | 3.2 | $\begin{bmatrix}6.4\\0\end{bmatrix}$ | $\begin{bmatrix}0\\-\frac{2}{5}\end{bmatrix}$ | $\begin{bmatrix}1\\0\end{bmatrix}$ |
| | | | | | | eqs. (23-24) is true with $\boldsymbol{r}^1 = \begin{bmatrix}0\\0\end{bmatrix}$ | | | | |

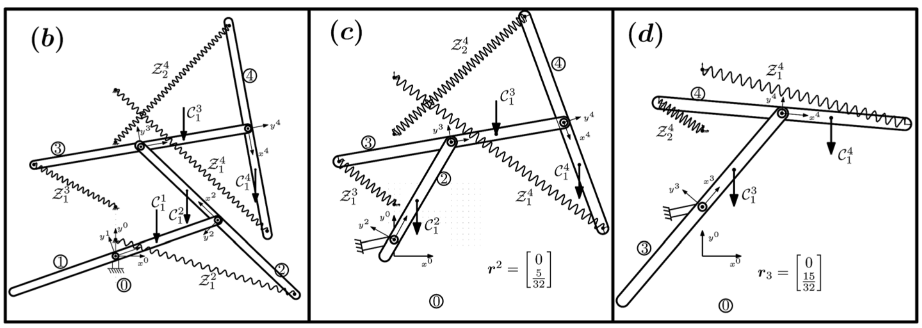


**Fig. 7 Details of statically balanced gravity loaded 4R linkage and its modification into 3R and 2R linkage.**

$\Phi_1^4(\mathcal{C}_1^4)$. There is no potential energy function of the second kind ($n_c^4 = 0$). Two zero-free-length springs $\mathcal{Z}_1^4$ and $\mathcal{Z}_2^4$ are added so that the functions $\Phi_1^4(\mathcal{C}_1^4)$, $\Phi_2^4(\mathcal{Z}_1^4)$, and $\Phi_3^4(\mathcal{C}_2^4)$ satisfy Eqs. (19)–(21) as per case (a) of step 1. All the details of the springs, constant loads as well as their potential energy in the standard form (see Eq. (15)) are presented in the table of Fig. 7. Now, as per step 2, the sum of $\Phi_1^4(\mathcal{C}_1^4)$, $\Phi_2^4(\mathcal{Z}_1^4)$, and $\Phi_3^4(\mathcal{Z}_2^4)$ is transformed as a $\Phi_2^3(\boldsymbol{r}^3, \theta^3)$ in accordance with Eq. (30) of Proposition (4.1). This is followed by making of a new tree-structure by deleting node 4 and associating $\Phi_2^3$ with node 3 of the new tree-structure. This completes the first iteration. The second iteration acts on the new tree-structure. The table in Fig. 7 and Fig. 7(*a*) give all the details of all the iterations. At the end of four iterations we are left with a single root node having constant function $\Phi_1^0$ associated with it. By following the dashed arrowed line of the Fig. 7(*a*) in the reverse order, it may be verified that

$$\Phi_1^0 = \Phi_1^1(\mathcal{C}_1^1) + \Phi_1^2(\mathcal{C}_1^2) + \Phi_1^3(\mathcal{C}_1^3) + \Phi_1^4(\mathcal{C}_1^4) + \Phi_2^4(\mathcal{Z}_1^4) + \Phi_3^4(\mathcal{Z}_2^4) + \Phi_3^3(\mathcal{Z}_1^3) + \Phi_3^2(\mathcal{Z}_1^2) \qquad (32)$$

Hence $\mathcal{C}_1^4$, $\mathcal{C}_1^3$, $\mathcal{C}_1^2$, and $\mathcal{C}_1^1$ are in static balance with $\mathcal{Z}_1^4$, $\mathcal{Z}_2^4$, $\mathcal{Z}_1^3$, and $\mathcal{Z}_1^2$.

To verify the static balance, this linkage along with the loads was modeled in ADAMS. With zero damping, a pulse of energy was initially introduced to the system. When the dynamic simulation of the system was carried out it was noticed that the net kinetic energy was constant over time. This implies that there was no potential gradient along the path that the linkage took in the dynamic simulation.

In Fig. 7(*c*), joint 1 and body 1 are eliminated to modify this 4R example into a 3R example. Joint 2 now joins body 2 with the ground at $\boldsymbol{r}^2 = \begin{bmatrix}0\\\frac{5}{32}\end{bmatrix}$. Rest of the bodies and their numbering is unchanged. The first two iterations for this example are identical to the 4R example. The third iteration is the last since node 2 now is a child of the root. As required at this iteration, it may be verified that Eqs. (23) and (24) are satisfied with $\boldsymbol{r}^2 = \begin{bmatrix}0\\\frac{5}{32}\end{bmatrix}$. One can have a similar modification of 4R example into a 2R example as shown in Fig. 7(*d*).

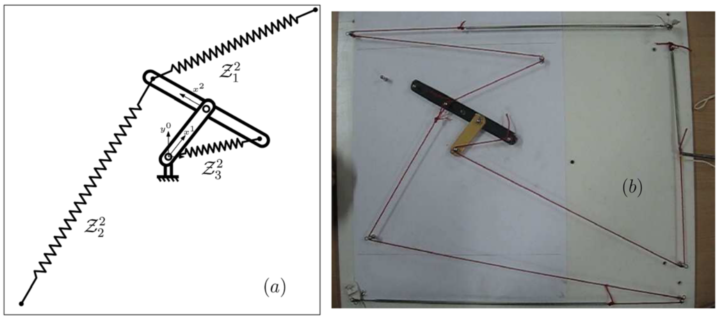


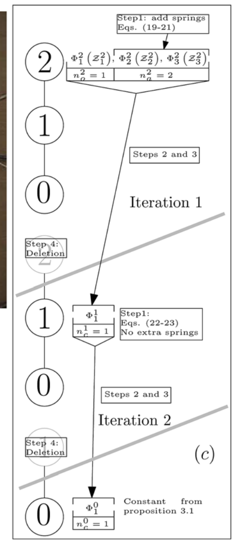


| no. | $\Phi_i^j$ | $\boldsymbol{a}_k^j$ | $\boldsymbol{b}_k^j$ | $k_k^j$ | $\rightarrow$ | $\boldsymbol{u}_i^j$ | $\kappa_i^j$ | $\boldsymbol{v}_i^j$ | $\boldsymbol{w}_i^j$ | $\boldsymbol{q}_i^j$ |
|---|---|---|---|---|---|---|---|---|---|---|
| 1 | $\Phi_1^2(\mathcal{Z}_1^2)$ | $\begin{bmatrix}5\\0\end{bmatrix}$ | $\begin{bmatrix}12\\12\end{bmatrix}$ | 1 | eq.(17) | $\begin{bmatrix}-12\\-12\end{bmatrix}$ | 0.5 | $\begin{bmatrix}5\\0\end{bmatrix}$ | $\begin{bmatrix}-12\\-12\end{bmatrix}$ | $\begin{bmatrix}5\\0\end{bmatrix}$ |
| 2 | $\Phi_2^2(\mathcal{Z}_2^2)$ | $\begin{bmatrix}5\\0\end{bmatrix}$ | $\begin{bmatrix}-12\\-12\end{bmatrix}$ | 1 | eq.(17) | $\begin{bmatrix}12\\12\end{bmatrix}$ | 0.5 | $\begin{bmatrix}5\\0\end{bmatrix}$ | $\begin{bmatrix}12\\12\end{bmatrix}$ | $\begin{bmatrix}5\\0\end{bmatrix}$ |
| 3 | $\Phi_3^2(\mathcal{Z}_3^2)$ | $\begin{bmatrix}-5\\0\end{bmatrix}$ | $\begin{bmatrix}0\\0\end{bmatrix}$ | 2 | eq.(17) | $\begin{bmatrix}0\\0\end{bmatrix}$ | 1 | $\begin{bmatrix}-10\\0\end{bmatrix}$ | $\begin{bmatrix}0\\0\end{bmatrix}$ | $\begin{bmatrix}-10\\0\end{bmatrix}$ |
| | | | $\sum_{i=1}^{3}\boldsymbol{u}_i^2 = \begin{bmatrix}0\\0\end{bmatrix}$ | | | | $\sum_{i=1}^{3}\kappa_i^3 = 2$ | | eqs. (19-21) true | |
| 4 | $\Phi_1^1$ | $\boldsymbol{s}_2^1 =$ | $\begin{bmatrix}1\\0\end{bmatrix}$ | | eq.(30) | $\begin{bmatrix}0\\0\end{bmatrix}$ | 2 | $\begin{bmatrix}20\\0\end{bmatrix}$ | $\begin{bmatrix}0\\0\end{bmatrix}$ | $\begin{bmatrix}5\\0\end{bmatrix}$ |
| | | | | | eqs. (23-24) is true with $\boldsymbol{r}^1 = \begin{bmatrix}0\\0\end{bmatrix}$ | | | | | |

**Fig. 8 Details of static balance of a 2R linkage under spring load**

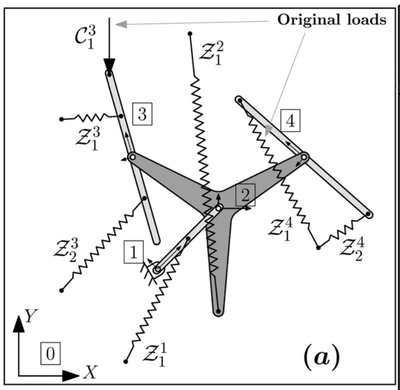


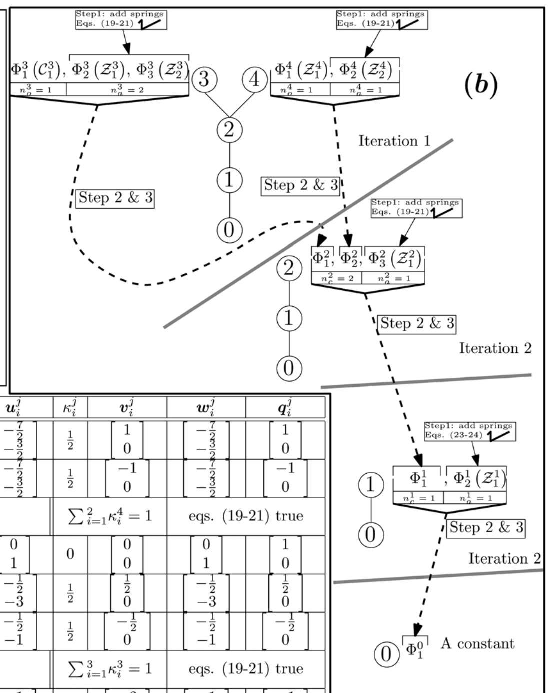


| no. | $\Phi_i^j$ | $\boldsymbol{a}_k^j/\boldsymbol{p}_k^j$ | $\boldsymbol{b}_k^j/\boldsymbol{f}_k^j$ | $k_k^j$ | $\rightarrow$ | $\boldsymbol{u}_i^j$ | $\kappa_i^j$ | $\boldsymbol{v}_i^j$ | $\boldsymbol{w}_i^j$ | $\boldsymbol{q}_i^j$ |
|---|---|---|---|---|---|---|---|---|---|---|
| 1 | $\Phi_1^4(\mathcal{Z}_1^4)$ | $\begin{bmatrix}1\\0\end{bmatrix}$ | $\begin{bmatrix}\frac{7}{2}\\\frac{3}{2}\end{bmatrix}$ | 1 | eq.(17) | $\begin{bmatrix}-\frac{7}{2}\\-\frac{3}{2}\end{bmatrix}$ | $\frac{1}{2}$ | $\begin{bmatrix}1\\0\end{bmatrix}$ | $\begin{bmatrix}-\frac{7}{2}\\-\frac{3}{2}\end{bmatrix}$ | $\begin{bmatrix}1\\0\end{bmatrix}$ |
| 2 | $\Phi_2^4(\mathcal{Z}_2^4)$ | $\begin{bmatrix}-1\\0\end{bmatrix}$ | $\begin{bmatrix}\frac{7}{2}\\\frac{3}{2}\end{bmatrix}$ | 1 | eq.(17) | $\begin{bmatrix}-\frac{7}{2}\\-\frac{3}{2}\end{bmatrix}$ | $\frac{1}{2}$ | $\begin{bmatrix}-1\\0\end{bmatrix}$ | $\begin{bmatrix}-\frac{7}{2}\\-\frac{3}{2}\end{bmatrix}$ | $\begin{bmatrix}-1\\0\end{bmatrix}$ |
| | | | $\sum_{i=1}^{2}\boldsymbol{u}_i^4 = \begin{bmatrix}-7\\-3\end{bmatrix}$ | | | | $\sum_{i=1}^{2}\kappa_i^4 = 1$ | | eqs. (19-21) true | |
| 3 | $\Phi_1^3(\mathcal{C}_1^3)$ | $\begin{bmatrix}1\\0\end{bmatrix}$ | $\begin{bmatrix}0\\-1\end{bmatrix}$ | | eq.(16) | $\begin{bmatrix}0\\1\end{bmatrix}$ | 0 | $\begin{bmatrix}0\\0\end{bmatrix}$ | $\begin{bmatrix}0\\1\end{bmatrix}$ | $\begin{bmatrix}1\\0\end{bmatrix}$ |
| 4 | $\Phi_2^3(\mathcal{Z}_1^3)$ | $\begin{bmatrix}\frac{1}{2}\\0\end{bmatrix}$ | $\begin{bmatrix}\frac{1}{2}\\3\end{bmatrix}$ | 1 | eq.(17) | $\begin{bmatrix}-\frac{1}{2}\\-3\end{bmatrix}$ | $\frac{1}{2}$ | $\begin{bmatrix}\frac{1}{2}\\0\end{bmatrix}$ | $\begin{bmatrix}-\frac{1}{2}\\-3\end{bmatrix}$ | $\begin{bmatrix}\frac{1}{2}\\0\end{bmatrix}$ |
| 5 | $\Phi_3^3(\mathcal{Z}_2^3)$ | $\begin{bmatrix}-\frac{1}{2}\\0\end{bmatrix}$ | $\begin{bmatrix}\frac{1}{2}\\1\end{bmatrix}$ | 1 | eq.(17) | $\begin{bmatrix}-\frac{1}{2}\\-1\end{bmatrix}$ | $\frac{1}{2}$ | $\begin{bmatrix}-\frac{1}{2}\\0\end{bmatrix}$ | $\begin{bmatrix}-\frac{1}{2}\\-1\end{bmatrix}$ | $\begin{bmatrix}-\frac{1}{2}\\0\end{bmatrix}$ |
| | | | $\sum_{i=1}^{3}\boldsymbol{u}_i^3 = \begin{bmatrix}-1\\-3\end{bmatrix}$ | | | | $\sum_{i=1}^{3}\kappa_i^3 = 1$ | | eqs. (19-21) true | |
| 7 | $\Phi_1^2$ | $\boldsymbol{s}_3^2 =$ | $\begin{bmatrix}-1\\\frac{3}{5}\end{bmatrix}$ | | eq.(30) | $\begin{bmatrix}-1\\-3\end{bmatrix}$ | 1 | $\begin{bmatrix}-2\\\frac{6}{5}\end{bmatrix}$ | $\begin{bmatrix}-1\\-3\end{bmatrix}$ | $\begin{bmatrix}-1\\\frac{3}{5}\end{bmatrix}$ |
| 8 | $\Phi_2^2$ | $\boldsymbol{s}_4^2 =$ | $\begin{bmatrix}1\\\frac{3}{5}\end{bmatrix}$ | | eq.(30) | $\begin{bmatrix}-7\\-3\end{bmatrix}$ | 1 | $\begin{bmatrix}2\\\frac{6}{5}\end{bmatrix}$ | $\begin{bmatrix}-7\\-3\end{bmatrix}$ | $\begin{bmatrix}1\\\frac{3}{5}\end{bmatrix}$ |
| 9 | $\Phi_3^2(\mathcal{Z}_1^2)$ | $\begin{bmatrix}0\\-\frac{6}{5}\end{bmatrix}$ | $\begin{bmatrix}2\\4\end{bmatrix}$ | 2 | eq.(17) | $\begin{bmatrix}-4\\-8\end{bmatrix}$ | 1 | $\begin{bmatrix}0\\-\frac{12}{5}\end{bmatrix}$ | $\begin{bmatrix}-2\\-4\end{bmatrix}$ | $\begin{bmatrix}0\\-\frac{12}{5}\end{bmatrix}$ |
| | | | $\sum_{i=1}^{3}\boldsymbol{u}_i^2 = \begin{bmatrix}-12\\-14\end{bmatrix}$ | | | | $\sum_{i=1}^{3}\kappa_i^2 = 3$ | | eqs. (19-21) true | |
| 10 | $\Phi_1^1$ | $\boldsymbol{s}_2^1 =$ | $\begin{bmatrix}1\\0\end{bmatrix}$ | | eq.(30) | $\begin{bmatrix}-12\\-14\end{bmatrix}$ | 3 | $\begin{bmatrix}6\\0\end{bmatrix}$ | $\begin{bmatrix}-12\\-14\end{bmatrix}$ | $\begin{bmatrix}1\\0\end{bmatrix}$ |
| 11 | $\Phi_2^1(\mathcal{Z}_1^1)$ | $\begin{bmatrix}\frac{1}{2}\\0\end{bmatrix}$ | $\begin{bmatrix}\frac{5}{4}\\\frac{1}{6}\end{bmatrix}$ | 12 | eq.(17) | $\begin{bmatrix}-15\\-2\end{bmatrix}$ | 6 | $\begin{bmatrix}6\\0\end{bmatrix}$ | $\begin{bmatrix}-\frac{5}{4}\\-\frac{1}{6}\end{bmatrix}$ | $\begin{bmatrix}6\\0\end{bmatrix}$ |
| | | | | | eqs. (23-24) is true with $\boldsymbol{r}^1 = \begin{bmatrix}\frac{13}{8}\\\frac{5}{4}\end{bmatrix}$ | | | | | |

**Fig. 9 Details of static balance of a 4R tree-structure linkage under a constant load and a spring load**

Illustration of the algorithm on a 2R linkage under a zero-free-length spring load: Just as Fig. 7 has every detail of the 4R example, Fig. 8 has every detail of this example. The explanation is also along the same lines of the previous example. In this example, the given original load is $\mathcal{Z}_1^2$ and the balancing loads are $\mathcal{Z}_2^2$ and $\mathcal{Z}_3^2$.

To buttress the fact that zero-free-length springs are practical, a prototype of this example was made, as shown in Fig. 8(*b*). To

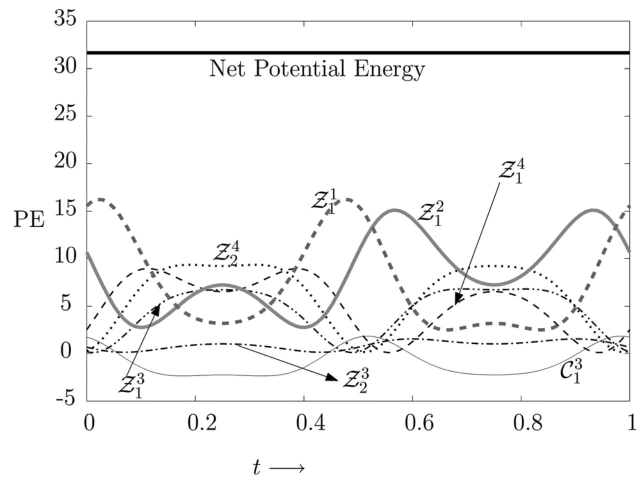


**Fig. 10 Potential Energy variation of spring loads, constant loads, and their sum**

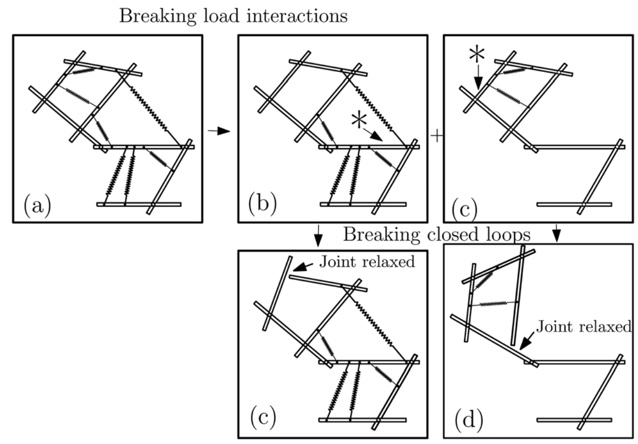


**Fig. 11 Breaking a problem as a superposition of several problem with each problem being static balance of revolute-jointed tree-structured linkage with loads exerted by the root body**

realize zero-free-length springs, pulley-string arrangement was used, the details of which can be found in Herder [5].

Illustration of the algorithm on a 4R tree-structure linkage under both constant load and zero-free-length spring load: While the previous two examples had serial architecture, this example has branches emanating form the same node, as shown in Fig. 9(*a*). The original loads acting on it are $\mathcal{C}_1^3$ and $\mathcal{Z}_1^4$. Instead of taking original loads to be exclusively constant loads or exclusively zero-free-length spring loads, here we have taken a combination of both types of loads. These original loads are balanced by adding springs $\mathcal{Z}_1^3$, $\mathcal{Z}_2^3$, $\mathcal{Z}_2^4$, $\mathcal{Z}_1^2$, and $\mathcal{Z}_1^1$ at various iterations in the iterative algorithm. A pictorial depiction of the iterations on these linkages is given in Fig. 9(*b*). All the remaining details are given in the table of the same figure.

To verify the static balance, $\theta$ s of bodies 1–4 are varied in the following form: $\theta^1 = \frac{\pi}{4} + \pi\sin(2\pi t)$, $\theta^2 = \frac{\pi}{12} + \pi\sin(2\pi t)$, $\theta^3 = \frac{\pi}{1.7} + \pi\sin(2\pi t)$, $\theta^4 = \frac{\pi}{1.3} + \pi\sin(2\pi t)$. The potential energy variation of original loads $\mathcal{C}_1^3$ and $\mathcal{Z}_1^4$ as well as the balancing loads, i.e., $\mathcal{Z}_1^3$, $\mathcal{Z}_2^3$, $\mathcal{Z}_2^4$, $\mathcal{Z}_1^2$, and $\mathcal{Z}_1^1$, are plotted in Fig. 10. The sum of all these variations is also plotted and it has turned out to be a constant. This verifies the static balance.

**4.3 Static Balancing of Any Revolute-Jointed Linkages With Any Kind of Zero-Free-Length Spring and Constant Load Interaction Within the Linkage.** In the static balancing method for linkages provided in Sec. 4.2, other than the fact that the linkage to be balanced has to be revolute-jointed and that load interactions are of zero-free-length spring or constant loads, there were two more restrictions as follows:

(1) It should be possible to consider that the loads on all the bodies are exerted by a common reference body (or frame) of the linkage.
(2) The linkage should have a tree-structure (i.e., without closed loops).

When the first restriction is violated as in Fig. 11(*a*), it is always possible to break the load interactions into a superposition of several load sets with each set complying to the first restriction. For example, the load interaction in Fig. 11(*a*) is broken into two load sets in Figs. 11(*b*) and 11(*c*). The reference body in each of these sets is indicated by an asterisk symbol (*) in its respective figure. Furthermore, in a load set, if there are closed loops, then the closed loops can be broken by relaxing certain joint constraints. Figures 11(*c*) and 11(*d*) illustrates breaking of closed loops respectively in Figs. 11(*b*) and 11(*c*). With closed loops broken, each of the load sets comply with the two restrictions and they can be statically balanced by adding balancing loads as per Sec. 4.2.

Once each of the load sets is balanced, the joint constraints that were relaxed for breaking closed loops can be reimposed without disturbing the static balance. In other words, when the potential energy that is a function of the configuration space is a constant, it remains as the constant even when the configuration space is restricted (due to re-attachment of the broken joints).

Once the constraints are reimposed, the linkages in all the load sets are the same as the original linkage and the loads on all the sets can be superposed. Since each load set is in static balance, the superposition is also in static balance. In other words, the sum of several constant potential energy functions due to several load sets is also a constant. This superposition contains all the original loads on the given linkage. The remnant loads in this superposition are the additional loads that balance the original loads. In this way, additional loads that statically balance any revolute-jointed linkage with zero-free-length spring and constant load interactions between the bodies of the linkage can always be found.

## 5 Static Balance of Spatial Linkages Having Zero-Free-Length Spring and Constant Load Interactions Within the Linkage

The static balancing technique of Sec. 4 was based on Proposition 4.1, which was presented for two planar bodies, with the revolute joints only serving to satisfy the condition 1 of the proposition. We can have analogous static balancing technique for spherical and revolute-jointed *spatial* linkages with zero-free-length spring and constant load interactions between the bodies of the linkage provided that

(1) the potential energy for zero-free-length spring and constant loads has the same form as given in Eq. (25),
(2) Proposition 4.1 is true even if the two bodies ($l$ and $j$) are free to move in space,
(3) spherical and revolute joints ensure condition 1 of Proposition 4.1, and
(4) analogous to constraints (19)–(21) which enable satisfying condition 3 of the Proposition 4.1, there are constraint equations for spatial case that a body can satisfy in practice, possibly by addition of extra zero-free-length spring loads.

The first one is true since in the derivation of the potential energy of constant loads in Eq. (1) and zero-free-length spring loads in Eq. (6) would require no modification even if $\boldsymbol{r}$ were to be considered as a spatial global coordinate ($3 \times 1$ matrix), $\boldsymbol{a}$, $\boldsymbol{b}$, $\boldsymbol{p}$ were to be considered as spatial local coordinates, and $\boldsymbol{R}(\theta)$ were to be considered as the spatial rotation matrix of the bodies with $\theta$ possibly representing Euler angles. That $\boldsymbol{R}^T\boldsymbol{R}$ is the identity matrix, which was used in the derivation, is true in the spatial case also.

The second one is true since Proposition 4.1 relies on Eq. (27), that $\boldsymbol{R}^T\boldsymbol{R}$ is the identity matrix, and matrix-algebraic manipulations. All of them are valid in the spatial case also.

The third one is true since a spherical joint ensures a common point between the two bodies it joins and a revolute joint ensures a common line between the two bodies it joins.

In the fourth one, the constraints (19)–(21) were obtained by expressing the potential energy as a linear combination of a set of basis functions involving $\boldsymbol{r}$ and $\theta$ and setting the coefficient of $\theta$-dependent basis functions to zero. In a similar vein, in the spatial case also, the potential energy would be a linear combination of a set of basis functions involving $\boldsymbol{r}$ and rotation defining, say, Euler angles. By setting the coefficients of Euler angle-dependent terms to zero, the analogous spatial constraints can be obtained. The claim that we are not substantiating in this paper, for the sake of brevity, is that these analogous constraint equations can also be satisfied in practice, if necessary with the addition of extra zero-free-length springs.

Thus, the static balancing technique presented in the paper for revolute-jointed planar linkages extends to spherical and revolute-jointed spatial linkages.

## 6 Conclusion

We presented a technique to statically balance any planar revolute-jointed linkage having zero-free-length spring and constant load interactions between the bodies of the linkage. The technique involves only addition of zero-free-length springs but not any extra link, unlike spring-aided perfect static balancing techniques currently in the literature. The technique extends to spatial spherical and revolute-jointed linkages as well. The technique relies on a recursive relation to iteratively remove the dependence of the potential energy on the configuration variables of the bodies of the linkage. Recognizing the recursive relation along with the minimal conditions that enable it constitutes the main contribution of this paper.

## Appendix A: Perfect Static Balance and Positive-Free-Length Springs

This is an appendix to Sec. 2. Here, the difficulty in achieving perfect static balance of a lever by using normally available positive-free-length springs is discussed.

The $\boldsymbol{d}^T\boldsymbol{d}$ term in the potential energy expression of a spring given in Eq. (5) was seen to be a linear combination of sin $\theta$, cos $\theta$ and 1 when expanded as in Eq. (6). Hence, by writing $\boldsymbol{d}^T\boldsymbol{d}$ as $\alpha$ sin $\theta$ $+\beta$ cos $\theta+\gamma$, the potential energy expression of the spring becomes:

$$\left(\frac{k}{2}(\alpha\sin\theta+\beta\cos\theta+\gamma)-kl_0\sqrt{(\alpha\sin\theta+\beta\cos\theta+\gamma)}+\frac{k}{2}l_0^2\right) \tag{33}$$

The first term in Eq. (33) is the zero-free-length part and the second term is the free-length part. If the free-length is positive, i.e., $l_0>0$, then the free-length part is negative. The free-length part of the spring is nonconstant (i.e., $k\neq 0$ and not both $\alpha$ and $\beta$ is zero) except for trivial situations where spring constant is zero or the spring is attached to the pivot of the lever. When there are several but finite positive-free-length and nontrivial springs, the net contribution of the free-length part is negative, and it is also not known have the possibility of being a constant, unlike the zero-free-length part. Furthermore, the free-length part is also not known to be in the function space spanned by sin $\theta$ and cos $\theta$. Hence, the possibility of free-length part cancelling (modulo a constant) with zero-free-length part is also ruled out. Thus, with several positive-free-length springs, there is no way the net potential energy could become a constant.

## Appendix B: Constraints Can be Satisfied, If Not as It Is, by Addition of Extra Zero-Free-Length Spring Loads

**Appendix B.1: Satisfying Constraints (12)–(14).** This appendix demonstrates how by adding extra zero-free-length spring loads constraints (12)–(14) can be satisfied. To differentiate between original loads and balancing loads, let $n_{s,o}$ and $n_{s,b}$ respectively represent the number of original and balancing zero-free-length spring loads with $n_{s,o}+n_{s,b}=n_s$. Also, let the spring loads be indexed such that the first $n_{s,o}$ loads are original loads with the remaining being balancing loads. Similar meaning applies for $n_{c,o}$ and $n_{c,b}$.

Case 1: Original loads violate the constraint (14), and balancing loads are only zero-free-length springs. Let us try to satisfy all the constraints by adding a single zero-free-length spring. As per the notation, this spring gets the index $i=n_{s,o}+1$. The constraint (14) can be written as follows:

$$k_{n_{s,o}+1}\boldsymbol{a}_{n_{s,o}+1}=-\sum_{i=1}^{n_{s,o}}k_i\boldsymbol{a}_i \tag{34}$$

where the known quantities related to original loads are on the right hand side. Equation (34) gives the unique solution of $k_i\boldsymbol{a}_i$ for $i=n_{s,o}+1$ to the constraint (14). Furthermore, the constraints (12) and (13) can be rewritten as

$$\left(\begin{bmatrix} k_ia_{x,i} & k_ia_{y,i} \\ -k_ia_{y,i} & k_ia_{x,i}\end{bmatrix}\begin{bmatrix} b_{x,i} \\ b_{y,i}\end{bmatrix}\right)_{i=n_{s,o}+1} = \begin{bmatrix} -\sum_{i=1}^{n_c}\left((f_{y_i}p_{y,i}+f_{x,i}p_{x,i})\right)-\sum_{i=1}^{n_{s,o}}\left(k_i(a_{y,i}b_{y,i}+a_{x,i}b_{x,i})\right) \\ +\sum_{i=1}^{n_c}\left((f_{x,i}p_{y,i}-f_{y,i}p_{x,i})\right)-\sum_{i=1}^{n_{s,o}}\left(k_i(a_{x,i}b_{y,i}-a_{y,i}b_{x,i})\right)\end{bmatrix} \tag{35}$$

The $2\times 2$ matrix on the left hand side of the equations is known since $k_i\boldsymbol{a}_i$ for $i=n_{s,o}+1$ is already solved in Eq. (34). Furthermore, the matrix is nonsingular since the right hand side of Eq. (34) that is the same as $k_{ns,o\,+\,1}\boldsymbol{a}_{ns,o\,+\,1}$ is *nonzero as per the description this case*. We take $\begin{bmatrix} b_{x,i} & b_{y,i}\end{bmatrix}^T$ for $i=n_{s,o}+1$ as the inverse of the $2\times 2$ matrix times the right hand side of the Eq. (35) so that the constraints (12) and (13) can also be satisfied. Thus, theoretically, with a single additional zero-free-length spring, all three constraints (12)–(14) can be satisfied.

Case 2: Original loads satisfy (14), but violate atleast one of the constraints (12) and (13). Balancing loads are only zero-free-length springs.

If we proceed along the same lines as the previous case, then in Eq. (35), the $2\times 2$ matrix on the left hand side becomes singular zero-matrix whereas the right hand side is nonzero by the description of the case. Thus, in this case, with a single balancing zero-free-length spring, it is not possible to satisfy the related constraint. However, it may be verified that by adding two balancing springs, all the constraints can be satisfied.

The cases 1 and 2 cover all possible types of constraint violation. Hence we assert that if the constraints are not satisfied as it is, then by adding a minimum of one zero-free-length spring in case (1) (the component related to original loads in constraint (14) is nonzero) and two zero-free-length spring in case (2) (the component related to original loads in constraint (14) is zero), the constraints can be satisfied.

**Appendix B.2: Satisfying Constraints (19)–(21)** In Appendix B.1, if the constraints (12)–(14) are respectively substituted by constraints (19)–(21), there is going to be no change except for the right hand side of Eq. (34) which takes the form $-\sum_{i=1}^{n_o} \boldsymbol{v}_i$, and the right hand side of Eq. (35) which takes the form $-\left[\sum_{i=1}^{n}\left(q_{y,i}w_{y,i}+q_{x,i}w_{x,i}\right) \quad \sum_{i=1}^{n}\left(q_{x,i}w_{y,i}-q_{y,i}w_{x,i}\right)\right]^T$. There is no change in the left hand side since here also, the additional loads are zero-free-length springs. Hence, analogous to the conclusion of Appendix B.1, we conclude that if the constraints (19)–(21) are not satisfied as it is, then by addition of a minimum of one zero-free-length spring in case the constraint (21) is originally violated and a minimum of two zero-free-length springs in case the constraint (21) is not originally violated, the three constraints can be satisfied.

## References


[1] Lucien LaCoste, www.http://en.wikipedia.org/wiki/Lucien_LaCoste

[2] Streit, D. A., and Shin, E., 1993, "Equilibrators for Planar Linkages," Trans. ASME J. Mech. Des., **115**(3), pp. 604–611.

[3] Fattah, A., and Agrawal, S. K., 2006, "Gravity-Balancing of Classes of Industrial Robots," *Proceedings of the 2006 IEEE International Conference on Robotics and Automation*, May 15–19, Orlando, Florida, pp. 2872–2877.

[4] Agrawal, S. K., and Fattah, A., 2004, "Gravity-Balancing of Spatial Robotic Manipulators," Mech. Mach. Theory, **39**(12), pp. 1331–1344.

[5] Herder, J. L., 2001, "Energy-Free Systems: Theory, Conception and Design of Statically Balanced Spring Mechanisms," Ph.D. thesis, Delft University of Technology, Delft, Netherlands.

[6] Cho, C., Lee, W., and Kang, S., 2010, "Static Balancing of a Manipulator With Hemispherical Work Space," *2010 IEEE/ASME International Conference on Advanced Intelligent Mechatronics (AIM)*, pp. 1269–1274.

[7] Zhang, D., Gao, F., Hu, X., and Gao, Z., 2011, "Static Balancing and Dynamic Modeling of a Three-Degree-of-Freedom Parallel Kinematic Manipulator," *2011 IEEE International Conference on Robotics and Automation (ICRA)*, pp. 3211–3217.

[8] Rahman, T., Ramanathan, R., Seliktar, R., and Harwin, W., 1995, "A Simple Technique to Passively Gravity-Balance Articulated Mechanisms," ASME J. Mech. Des., **117**(4), pp. 655–658.

[9] Lin, P.-Y., Shieh, W.-B., and Chen, D.-Z., 2010, "Design of a Gravity-Balanced General Spatial Serial-Type Manipulator," ASME J. Mech. Rob., **2**, 031003.

[10] Herder, J. L., 1998, "Design of Spring Force Compensation Systems," Mech. Mach. Theory, **33**(1-2), pp. 151–161.

[11] Deepak, S. R., and Ananthasuresh, G. K., 2012, "Static Balancing of a Four-Bar Linkage and Its Cognates," Mech. Mach. Theory, **48**(0), pp. 62–80.

[12] Deepak, S. R., and Ananthasuresh, G. K., 2009, "Static Balancing of Spring-Loaded Planar Revolute-Joint Linkages Without Auxiliary Links," *14th National Conference on Machines and Mechanisms*, Dec. 17–18, NIT Durgapur, India.

[13] Lin, P.-Y., Shieh, W.-B., and Chen, D.-Z., 2010, "A Stiffness Matrix Approach for the Design of Statically Balanced Planar Articulated Manipulators," Mech. Mach. Theory, **45**, pp. 1877–1891.

[14] Agrawal, A., and Agrawal, S., 2005, "Design of Gravity Balancing Leg Orthosis Using Non-Zero Free Length Springs," Mech. Mach. Theory, **40**, pp. 693–709.

[15] Gopalswamy, A., Gupta, P., and Vidyasagar, M., 1992, "A New Parallelogram Linkage Configuration for Gravity Compensation Using Torsional Springs," *Proceedings of the 1992 IEEE International Conference on Robotics and Automation*.

[16] Gosselin, C. M., and Wang, J., 2000, "Static Balancing of Spatial Six-Degree-of-Freedom Parallel Mechanisms With Revolute Actuators," J. Rob. Syst., **17**(3), pp. 159–170.

[17] Ulrich, N., and Kumar, V., 1991, "Passive Mechanical Gravity Compensation for Robot Manipulators," *Proceedings of the 1991 IEEE International Conference on Robotics and Automation*, Vol. 2, pp. 1536–1541.

[18] Endo, G., Yamada, H., Yajima, A., Ogata, M., and Hirose, S., 2010, "A Passive Weight Compensation Mechanism With a Non-Circular Pulley and a Spring," *2010 IEEE International Conference on Robotics and Automation (ICRA)*, pp. 3843–3848.

[19] Koser, K., 2009, "A Cam Mechanism for Gravity-Balancing," Mech. Res. Commun., **36**(4), pp. 523–530.

[20] de Visser, H., and Herder, J. L., 2000, "Force-Directed Design of a Voluntary Closing Hand Prosthesis," J. Rehabil. Res. Dev., **37**, pp. 261–271.

[21] Herder, J. L., and van den Berg, F. P. A., 2000, "Statically Balanced Compliant Mechanisms (SBCMS), an Example and Prospects," *Proceedings ASME DETC 26th Biennial Mechanisms and Robotics Conference*, Paper no. DETC2000/MECH-14144.

[22] Howell, L. L., and Midha, A., 1995, "Parametric Deflection Approximations for End-Loaded, Large-Deflection Beams in Compliant Mechanisms," ASME J. Mech. Des., **117**, pp. 156–165.

[23] Howell, L. L., 2001, *Compliant Mechanisms*, Wiley, New York.